Pergamon

D01F9/15

6026 Carbon
32(1994)No.2, Head.Hill Hall, Oxford, GB

p. 301-310 = (10)

D01F9/155

A PROCESSING WINDOW FOR INJECTION OF MESOPHASE PITCH INTO A FIBER PREFORM

J. L. WHITE, M. K. GOPALAKRISHNAN, and B. FATHOLLAHI
Department of Applied Mechanics and Engineering Sciences, University of California, San Diego; La Jolla, California 92093-0310

(*Received* 19 *July* 1993; *accepted in revised form* 16 *August* 1993)

Abstract—A review of viscosity data for mesophase pitches prepared by pyrolysis of petroleum or coal-tar pitches, or by chemical and thermal treatment of organic precursors ("chemical pitches"), finds that, although the apparent viscosities range widely, the temperature dependencies follow a regular pattern. Mesophase pitches prepared from petroleum or coal-tar precursors are very viscous, but can be used in a partially transformed state to obtain some reduction in viscosity; in contrast, most chemical pitches are less viscous at full transformation.

The processing window for injection of mesophase pitch into a fiber preform derives from three requirements: the mesophase must be fluid enough to avoid deformation of the preform, sufficiently stable to limit viscosity increase and bubble formation during injection, but high enough in softening point to permit oxidation stabilization.

Capillary flow measurements were used in selecting a mesophase pitch for injection through 2D preforms made by 45°-layup of a plain-weave carbon fabric. The viscosity of a decanted mesophase pitch prepared by partial transformation of a petroleum pitch was found to lie above the processing window. However an alkylbenzene-based mesophase pitch showed a favorable combination of viscosity and thermal stability; using injection temperatures near 310°C and driving pressures of 0.1 MPa, steady penetrating flow was obtained with good filling of fiber bundles.

Key Words—Mesophase pitch, capillary flow, viscosity, carbon–carbon composite, pitch injection.

1. INTRODUCTION

Two key steps in the fabrication of mesophase carbon fiber[1,2] are (a) the formation of highly oriented microstructures by extrusion and draw of pitch in the mesophase (liquid crystalline) state, and (b) stabilization by oxidation of the drawn filaments to prevent softening and structural relaxation during carbonization. Recent years have seen the preparation of fully transformed mesophase pitches of much lower viscosity than the pitches used in the original development of mesophase carbon fiber[3–7], and oxidation stabilization has been found applicable to mesophase in bulk if an adequate access porosity exists to permit oxidation in depth[8,9]. This paper reports on research[10–12] that seeks to use these developments to improve the fabrication of carbon materials.

Our focus is on injection of mesophase pitch into fiber preforms, where the mismatch in thermal expansivities of mesophase[13] and fiber favors the formation of interlinked shrinkage cracks that provide oxygen access throughout the composite body[8]. To attain fluidity adequate for effective flow and filling of the preform, the injection temperature must approach the limit of thermal stability of the pitch. These points constitute limitations framing a processing window[11] that may be used to select a mesophase pitch from the range of such pitches now becoming available. The selected pitch must be well suited for the steps of injection, stabilization, and carbonization that are required to fabricate a finished composite.

2. VISCOSITY OF MESOPHASE PITCH

Early in-situ measurements on petroleum or coal-tar pitch pyrolyzing within a rotating-cylinder rheometer at temperatures near 400°C showed that, although the torque increased rapidly as the isotropic pitch transformed to mesophase, for some pitches there was a time-limited window in which the pyrolyzing mass might be manipulated as a viscous anisotropic liquid[14,15]. Although analysis of flow in such a reactive two-phase liquid is complex[16,17], an apparent viscosity can be calculated from the torque after a steady state is reached, and this practical measure of flow behavior is relevant to such processes as injection or fiber-spinning of mesophase pitch.

A substantial body of such data is now available for mesophase pitches measured at temperatures well below those used in the thermal treatment for their preparation, and the data collected in Fig. 1 from Nazem and Lewis[3,18–20] and other sources[4,6,21,22] are relatively free of uncertainties concerning ongoing pyrolysis reactions during the viscosity measurements. Three types of precursor are distinguished here: petroleum pitch; coal-tar pitch, which may have been filtered or centrifuged to remove insoluble particles; and "chemical" pitch,

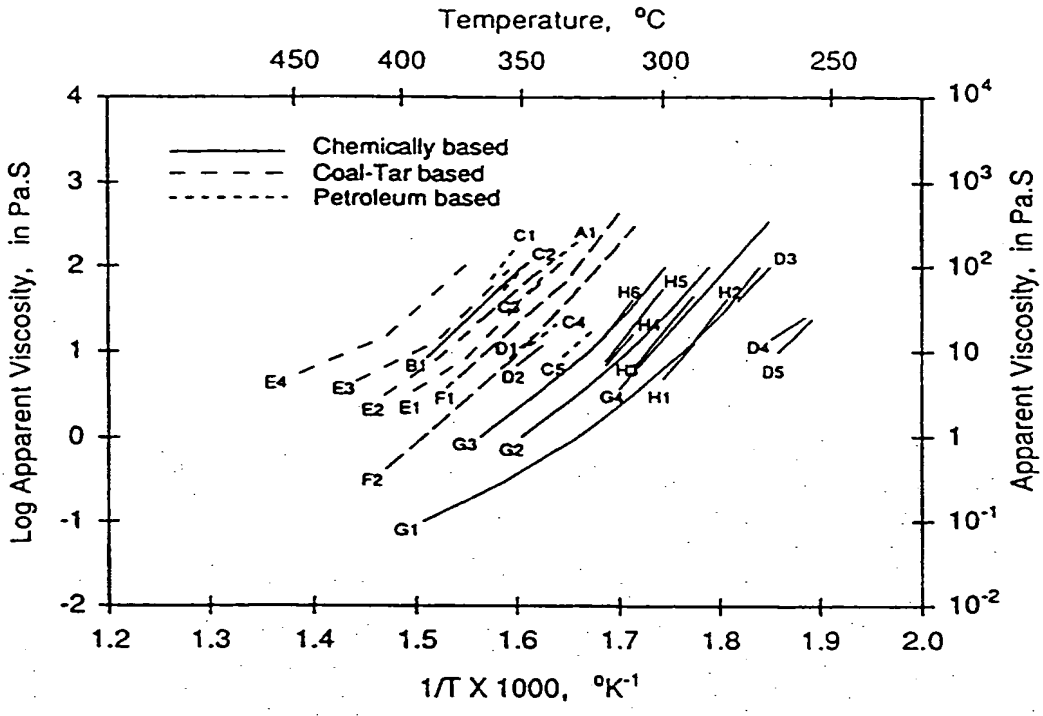

Fig. 1. Apparent viscosities of mesophase pitches. The symbols refer to Table 1 where the pitches are identified.

which may consist of the polymerization and pyrolysis of an aromatic hydrocarbon, often with the objective of controlling the molecular weight distribution. Table 1 indexes the viscosity data of Fig. 1 to the precursor and its preparation; in most cases an optical estimate of the extent of transformation to mesophase[25] as well as the Mettler softening point are reported.

For clarity, Fig. 1 is limited to results for which temperature dependencies are reported, and the data are plotted as the logarithm of the apparent viscosity as a function of inverse temperature. In this way similarities in temperature dependence become clear for pitches that range in viscosity over nearly four orders of magnitude. For cases where measurements were made over a lengthy temperature range, a tendency to decreased slopes at viscosities below about 10 Pa.s is also evident. In some cases such data are reported as a curve, in other cases as two straight lines with an abrupt change in activation energy; although this change in slope may signal a change in flow mechanism, our immediate interest lies simply in making reasonable extrapolations to a common temperature, as has been done for 325°C in Fig. 2; this figure includes extrapolations from some single-temperature viscosity measurements that were excluded from Fig. 1.

Figure 2 shows the decreased viscosity levels that can be realized if the pyrolysis of a petroleum or coal-tar pitch is stopped short of full transformation to mesophase. This approach was used in the early development of mesophase carbon fiber to produce more spinnable pitches[1]; by interrupting pyrolysis after the mesophase has become the continuous phase but before transformation is complete, the viscosity can be reduced by nearly two orders of magnitude. More striking in Fig. 2, however, are the yet lower levels of viscosity, even when fully transformed to mesophase, that can be attained with "chemical" pitches, as brought out by Lewis and Nazem[3].

3. THE PROCESSING WINDOW FOR MESOPHASE INJECTION

The data summarized in Fig. 1 and Table 1 provide the basis for sketching a schematic spectrum for the range of viscosities of various types of mesophase pitch, as shown in Fig. 3. Here three fields are distinguished by the precursor and its degree of transformation, each field bounded on its low-viscosity edge by:

AA': The lowest viscosity reported for a mesophase pitch prepared from petroleum or coal-tar pitch by pyrolysis to 100% mesophase.

BB': The lowest viscosity reported for a petroleum- or coal-tar-based mesophase pitch only partially transformed to mesophase.

Table 1. Viscosity measurements on mesophase pitch

S	Precursor and treatment	MSP	MC	E'_η	E'_η	Source
A1	Petroleum pitch: pyrolyzed[23]	NA	93	44.4		Nazem[18]
B1	Naphthalene: pyrolyzed	231	100	51.0		Nazem[19]
C1	Petroleum pitch: pyrolyzed at 390°C	339	96	71.2		Nazem and Lewis[20]
C2		334	89	58.8		
C3		329	83	56.4		
C4		324	80	45.7		
C5		312	66	48.2		
D1	Petroleum pitch: pyrolyzed	332	75	51		Lewis and Nazem[3]
D2	Naphthalene: pyrolyzed	329	100	43		
D3	Naphthalene: polymerized, pyrolyzed	254	100	56		
D4	Naphthalene-phenanthrene: pyrolyzed	244	100	35		
D5	D4, with liquid crystal additive	242	100	52		
E1	Coal-tar pitch: filtered, hydrogenated, and pyrolyzed	NA	100	54.3	32.7	Fitzer, Kompalik, and Yudate[21] Note 1
E2		NA	85	46.4	37.3	
E3		NA	95	52.8	27.0	
E4		NA	95	48.8	23.7	
F1	Coal-tar pitch: filtered, hydrogenated, and pyrolyzed	NA	NA	71.8	48.2	Yamada *et al.*[22] Note 1
F2		NA	NA	62.5	45.5	
G1	Naphthalene: pyrolyzed	252	100	Note 2		Ohtsuka, Mitsubishi Gas-Chemical Co. [6]
G2		272	100			
G3		281	100			
G4		NA	100	60.4		Yanagida *et al.* Mitsubishi Oil Co. [4]
H1	Alkylbenzenes: polymerized and pyrolyzed	260	100	61.4		
H2		261	100	67.0		
H3		270	100	64.9		
H4		280	100	60.1		
H5		282	100	66.4		
H6		289	100	64.9		
J1	Petroleum pitch: pyrolyzed and decanted[24]	NA	99	61.8		Present work, see Fig. 3
J2	Alkylbenzenes: same as H-series	280	100	56.4		Present work[12]

S Identifying symbol used in Figs. 1 and 3.
MSP Mettler softening point, °C.
MC Mesophase content, volume-%.
E_η, E'_η Activation energy for viscous flow, kilocalories/mol.
NA Not available.
Note 1 Viscosity reported as two straight-line segments.
Note 2 Viscosity reported as a concave-upward curve for log η *vs.* $1/T$.

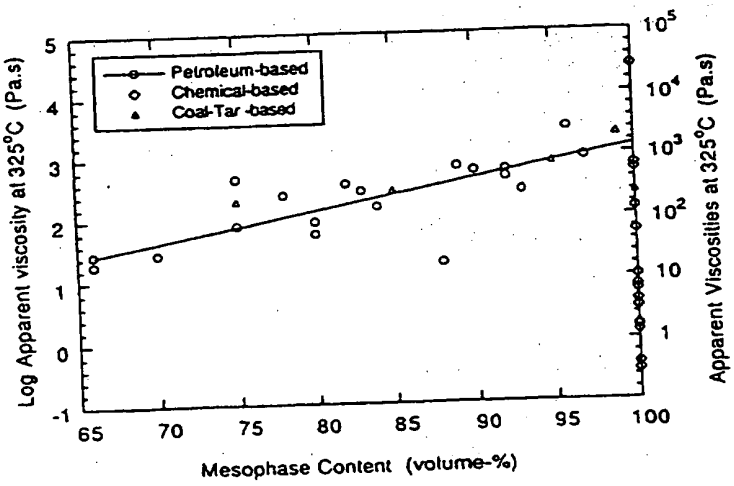

Fig. 2. Apparent viscosities of mesophase pitches at 325°C.

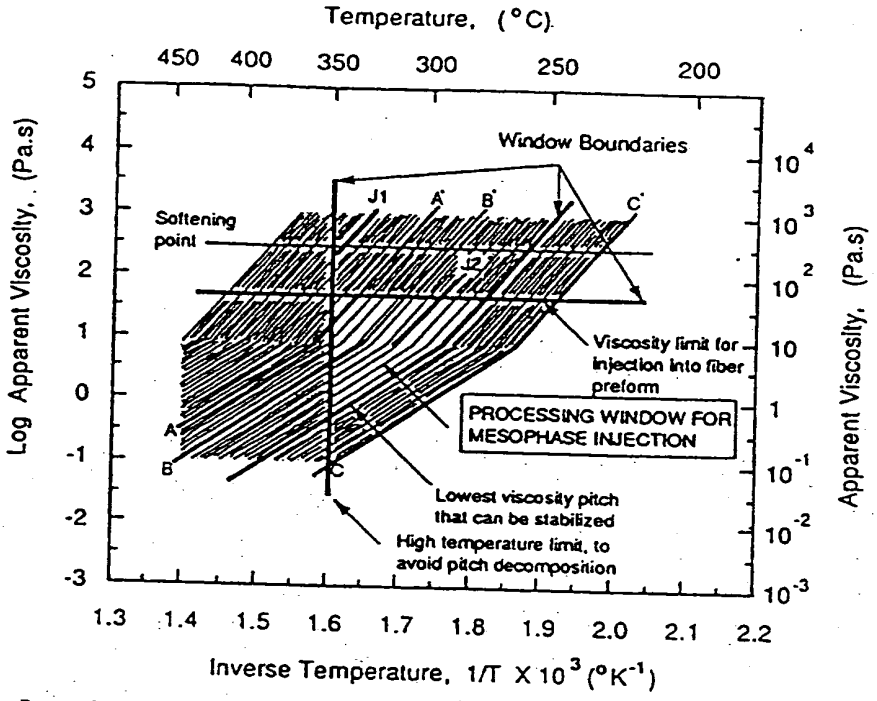

Fig. 3. Processing window for injection of mesophase pitch through a fiber preform, superposed on a schematic viscosity spectrum. Line AA′ refers to the lowest viscosity reported for petroleum- or coal-tar-based mesophase, fully transformed; BB′, same as AA′, but only transformed to mesophase as the continuous phase; and CC′, the lowest viscosity reported for chemically based mesophase pitch, in the fully transformed state. J1 and J2 locate measurements made in this study on a decanted mesophase (J1) prepared from petroleum pitch[24] and a chemical mesophase (J2) prepared from alkylbenzenes[4,5].

but with the mesophase acting as the continuous phase.

CC′: The lowest viscosity reported for a chemically derived, fully transformed mesophase pitch.

To construct Fig. 3, the viscosity of a mesophase pitch was assumed to be reasonably approximated on an Andrade plot ($\log \eta$ versus $1/T$) by two straight lines intersecting at a viscosity of 8 Pa.s. For simplicity, activation energies of 60 kcal/mol for $\eta_{hi} >$ 8 Pa.s and 35 kcal/mol for $\eta_{lo} <$ 8 Pa.s were also assumed; thus the Andrade viscosity functions used in Fig. 3 are:

$$\text{Log}\,\eta_{hi} = A_{hi} + \frac{13115}{T}, \qquad \text{(1a)}$$

$$\text{Log}\,\eta_{lo} = A_{lo} + \frac{7650}{T}. \qquad \text{(1b)}$$

An estimate for the viscosity of a mesophase pitch at its softening point can be made by extrapolating the Andrade function to the measured softening point. The average estimated viscosity at the Mettler softening point for the fully transformed mesophase pitches of Fig. 1 was found to be 300 Pa.s; this level is sketched into the viscosity spectrum as a means of estimating the position in the processing window of a pitch whose softening point is known, but for which more detailed viscosity data are not available.

Considering now the injection of mesophase pitch into a carbon fiber preform, a processing window may be superposed on the schematic viscosity spectrum based on three practical limitations:

1. An upper limiting viscosity determined by the permeability of the fiber preform and by the need to avoid injection pressures that could distort the preform; from experience with 2D preforms layed up from woven fabric, we choose conservatively an upper limiting viscosity of 50 Pa.s.
2. An upper limiting temperature determined by the need to avoid excessive thermal degradation of the pitch on the time scale of the injection process. This temperature will vary with the thermal stability of the pitch and the extent of degradation acceptable in the process. Thinking in terms of a petroleum-based mesophase pitch, we estimate this boundary at 350°C.
3. A lower limiting viscosity determined by the need to stabilize the matrix by oxidation after

the injection process is complete. Thus, the viscosity at the lowest practical temperature for oxidation, say 200°C, must be sufficiently high to resist softening that would close the shrinkage cracks that provide oxygen access and enable oxidation to proceed at depth within a composite[8]. This lower viscosity limit is sketched into Fig. 3 on the basis that fiber spun from a mesophase pitch with a softening point as low as 260°C can be stabilized by oxidation[4].

4. OBSERVATIONS OF MESOPHASE FLOW

4.1 *Experimental methods*

A schematic diagram of the pitch injection device used to study mesophase flow in capillaries or in 2D fiber preforms is shown in Fig. 4. This device can be assembled in two ways: to accommodate stainless steel capillary tubes that can be replaced with minimal disturbance; and to permit injection of pitch through a 2D layup of woven fabric plies. Tie rods, copper gaskets, and a torque wrench are used to ensure containment of nitrogen to pressures of at least 1 MPa. The structural components are made of stainless steel to resist corrosion at operating temperatures up to 450°C.

When used as a capillary viscometer, with capillaries of the order of one millimeter in internal diameter held by friction-fit in the copper quenching block, a capillary tube can be quenched when flow conditions have stabilized, and then removed for micrographic examination of the flow structures. When assembled for the injection of pitch through a 2D layup of woven fabric plies, a compression ring is used with shim rings between plies to restrict edgewise leakage from the fiber preform.

Temperature uniformity in this device is important because an activation energy near 60 kcal/mole corresponds to a viscosity sensitivity of 8%/°C. Stirring is effective in reducing thermal gradients but should be used with caution, especially at high viscosity levels, in view of the fine structure and preferred orientation that can be induced in the anisotropic liquid. Two sets of heaters, located above and below the flow or injection region, permit fine adjustment of heating power to equalize the temperatures observed at the thermocouple positions.

For micrographic examination, a diamond saw is used to cut transverse sections that are vacuum-impregnated with epoxy resin before proceeding to grinding on SiC papers. Fine grinding is done with mylar-backed alumina grinding sheets, using 9-micron and 3-micron grades. Rough polishing is done with one-micron diamond paste on a napless cloth, and the final polish is made by hand with 0.05-micron ceria.

4.2 *Decanted mesophase pitch derived from petroleum pitch*

Severe thermal treatments are usually needed to convert the last molecular components of a petroleum or coal-tar pitch to mesophase[26]; such processes risk the polymerization of more reactive components to large molecules that can contribute strongly to high viscosity. An approach that limits the thermal treatment comprises interruption of pyrolysis in the range of partial transformation and removal of the isotropic pitch by decanting. To learn where such a mesophase pitch lies relative to the processing window, a decanted mesophase pitch prepared at Aerotherm Corporation[24] from Ashland A240 petroleum pitch was studied in capillary flow.

After meltdown and stirring at 360°C to remove bubbles and to homogenize the mesophase pitch, a set of measurements at 330°C found a linear relation-

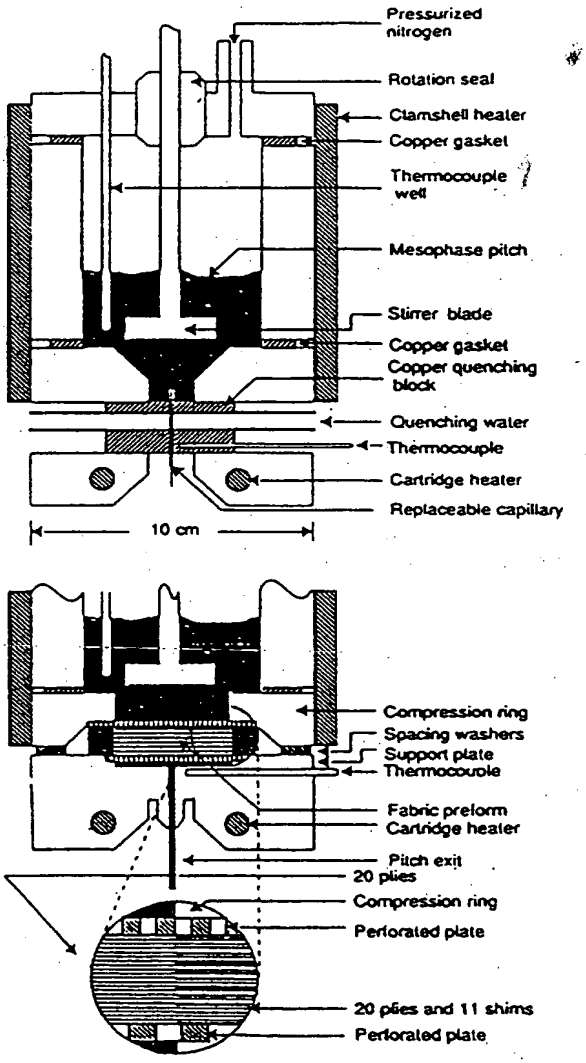

Fig. 4. Schematic diagram of pitch injection device: above, as assembled for capillary measurements; below, as assembled for injection of pitch into a 2D lay-up of 20 plies of carbon fabric. Inset shows how transverse leakage of pitch is limited by shims in an outer compression ring.

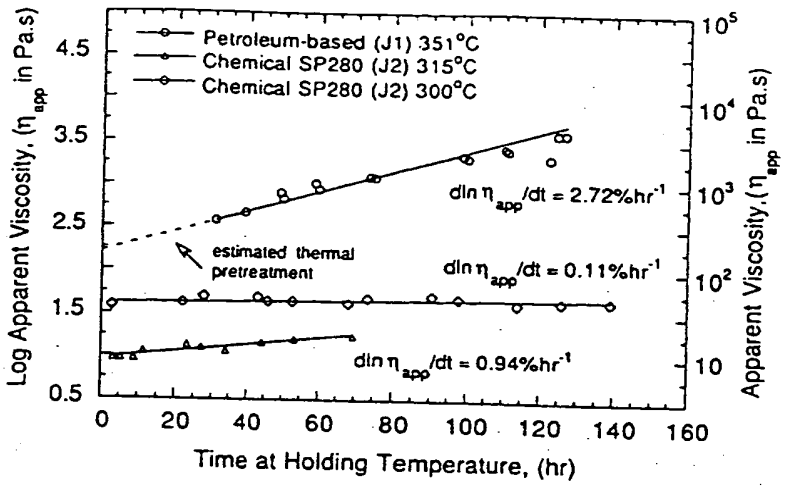

Fig. 5. Apparent viscosities of two mesophase pitches measured over lengthy periods to define the thermal instability.

ship between flow rate and applied pressure. The capillary measurements were then extended in two steps to 347°C to obtain the slope of the viscosity line labelled J1 in Fig. 3. Attempts to extend measurements to higher temperatures encountered thermal instability; Fig. 5 illustrates the increase in viscosity with time at 351°C for a specimen of the decanted mesophase pitch that had already experienced some thermal reaction in capillary runs attempted at higher temperatures.

The results showed that this mesophase pitch begins to display thermal instability at about 350°C, and it was estimated that the viscosity had been increased by about 23% by the homogenizing thermal treatment after meltdown. Using this correction, the capillary measurements give

Decanted Mesophase Pitch J1:

$$\text{Log}\,\eta(\text{Pa.s}) = \frac{13514}{T(^\circ\text{K})} - 19.4351, \quad (2)$$

which extrapolates to a value of 1440 Pa.s at 325°C, consistent with the viscosity of other petroleum-based mesophase pitches in Fig. 2. Since the viscosity level of the decanted mesophase pitch lies well above the processing window, our attention turned to chemically based pitches of lower viscosity.

4.3 *Mesophase pitch from alkylbenzenes*

To examine the suitability of chemically based mesophase pitches for injection processes, a pitch was selected from the low-softening-point series manufactured by the Mitsubishi Oil Company[4]. These pitches are prepared from alkylbenzenes by controlled polymerization and pyrolysis to yield fully transformed mesophase pitches with Mettler softening points as low as 230°C[5]. The Mitsubishi Oil Mesophase Pitch with a softening point of 280°C (specified as MOMP/SP280) was chosen for its position in the center of the processing window. A density of 1.2 g/cm^3[4] was assumed for the calculation of apparent viscosity from capillary flow measurements.

In capillary runs near 325°C, irregular flow rates were sometimes observed, and bubbles were found in quenched capillaries as well as in the pitch chamber, indicating that the stability limit of this pitch had been exceeded. Long-term capillary runs at lower temperatures, two of which are included in Fig. 5, found that a rising viscosity was measurable at temperatures as low as 300°C; however, the results also show that the alkylbenzene-based pitch MOMP/SP280 has a significant advantage in thermal stability at equivalent viscosities in comparison with the petroleum-based mesophase pitch. A thermal stability described by

$$\frac{d\ln\eta}{dt} < 1\frac{\%}{\text{h}} \quad \text{for } T < 315^\circ\text{C} \quad (3)$$

is sufficient to enable processing that does not risk long exposure of the pitch to temperatures above 315°C.

In a concurrent study[12], the capillary rheometer is used to study the flow parameters of MOMP/SP280 pitch and to define the microstructures induced by flow. To summarize results relevant to injection into fiber preforms, the apparent viscosity of this mesophase pitch is essentially independent of shear rate over 10 to 1000 s^{-1} in the temperature range of 290 to 315°C and can be represented by

MOMP/SP280 (J2):

$$\text{Log}\,\eta\,(\text{Pa.s}) = \frac{12322}{T(^\circ\text{K})} - 19.948 \quad (4)$$

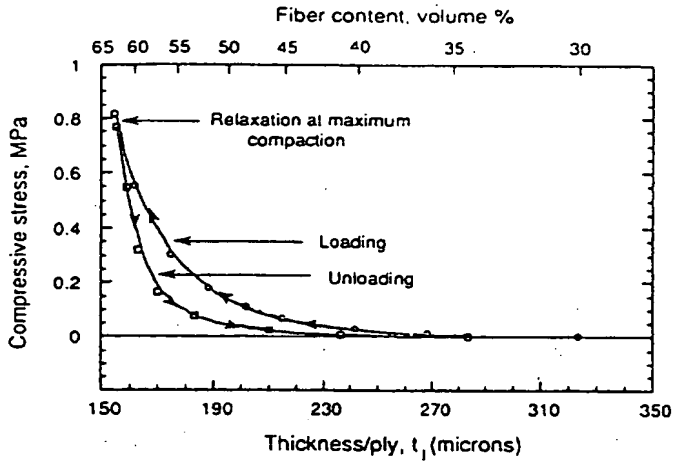

Fig. 6. Compaction and springback stresses for a 45°-lay-up of 19 plies of a plain-weave carbon fabric (Fiberite W-134G).

5. INJECTION OF MESOPHASE PITCH INTO 2D FIBER PREFORMS

5.1 *Experimental design*

The pitch injection device, configured as shown in the lower part of Fig. 4, was employed to force penetrating flow of mesophase pitch through 2D-layups of carbon fabric. A plain-weave fabric was chosen for its openness of weave: Fiberite W-134G fabric, woven from Amoco T-300 (3K) PAN-based carbon fiber and heat treated to 2150°C after weaving. The square weave of 12.5 by 12.5 strands per inch leaves a weave gap of nearly 0.7 mm. A 45°-layup was chosen because observations of light transmission through a pair of plies indicated that 45°-rotation from ply to ply produces a more reproducible and uniform pattern of channels for penetrating flow than does a warp-aligned lay-up.

Compaction measurements on a 2D-lay-up were used to dimension the compression ring and the shims layed-up with the fabric plies. The data of Fig. 6 refer to 19 plies of W-134G fabric, layed up with 45°-rotation from ply to ply, and tested in compression with 5-cm diameter anvils on an Instron 4204 mechanical test machine. On loading, the stress increases in a near-exponential manner as a limiting ply thickness near 150 microns is approached. Although some relaxation may occur while holding near this ply thickness, and the spring-back stress on unloading is seen to lag well below the loading stress, nearly the same compaction path is followed if the testing cycle is repeated.

The compaction data permit design of the spacing washers (see Fig. 4) and the preform thickness under the perforated plate to correspond to a compressive stress greater than the injection pressure; the intent is to minimize further compaction by the driving pressure and thus to maintain some control of the size of flow channels during injection. The shims placed between plies in the containment ring raise the stress in this ring well above the injection pressure, and edge leakage is reduced to a small fraction of the penetrating flow measured at the bottom outlet. Shims cut from 0.1-mm copper sheet or from the W-134G carbon fabric performed satisfactorily.

5.2 *Injection runs*

In commencing an injection run, a nitrogen purge through the bed of pitch particles above the preform is maintained during heating until gas flow is blocked by meltdown of the pitch. To minimize oxidation of the pitch, the device is heated rapidly to establish penetrating flow without delay.

In exploring injection conditions, the injection temperature, from 285 to 330°C, was taken as the primary variable; driving pressures were run as high as 100 psi, and the ply thicknesses were in the range of 200 to 250 microns.

As shown by Fig. 7, injection runs 315°C often found decreasing flow with time, with the decrease exceeding the rate that might be anticipated from the data of Fig. 5. Micrographic examination of sectioned specimens found bubbles in many of the flow channels (Fig. 8a), although the fiber bundles were usually well filled with mesophase (Fig. 8b). Polarized-light microscopy confirmed that the matrix morphology within the fiber bundles was determined primarily by the sheath effect[27]. Injection runs at temperatures below 315°C displayed steadier flow, and bubbles were infrequent in the flow channels. The conditions for the injection runs illustrated by Figs. 7 and 8 are summarized in Table 2.

Table 2 includes some permeability data calculated from the Darcy relationship,

$$\text{Permeability, } k = \frac{\dot{m}\eta n t_l}{A\rho\Delta P} \qquad (5)$$

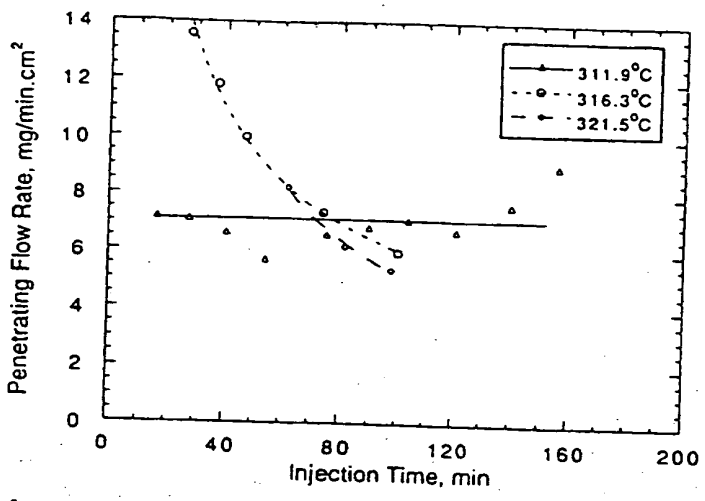

Fig. 7. Rates of mass flow of mesophase pitch through plain-weave preforms at three injection temperatures. Run conditions for the 45°-lay-ups are summarized in Table 2.

where $\dot{m}$ is the mass flow rate through area A, ρ is the density, nt_1 is the thickness of n plies, and ΔP is the injection pressure. For a given preform, the permeability was reproducible to ±5%, but for a set of eight nominally equivalent preforms, the permeabilities varied by ±50%. This observation provides a measure of the uniformity of flow that can be expected with a 45°-lay-up of plain-weave carbon fabric. Nevertheless the results in Table 2 indicate that the permeability is a strong function of the preform compaction.

6. DISCUSSION

The alkylbenzene-based mesophase pitches appear well-suited for injection into fiber preforms by offering good filling and high carbon yield upon stabilization and carbonization. Similar conclusions were reached by Fujiura *et al.*[7] in a recently completed investigation of the naphthalene-based mesophase pitches developed by Mochida *et al.*[6]. Thus, a fabricator of carbon materials now has a wide selection of low-viscosity fully anisotropic mesophase pitches that can be injected, stabilized, and graphitized to carbon yields higher than can be obtained with conventional binder pitches.

As a class, mesophase pitches produced by pyrolysis of petroleum or coal-tar pitch appear to be too viscous for use in the injection processes considered here. However, they may be well-suited for related processes, such as the warm-pressing of prepregged fiber bundles[9,28], where the flow distance required for successful processing is small.

The processing window, expressed in terms of apparent viscosity and temperature, illustrates three competitive requirements: the pitch must be sufficiently fluid to flow without excessive distortion of the preform, possess thermal stability adequate to complete the injection process, and yet be sufficiently viscous to retain the shrinkage-crack porosity essential to stabilization in depth by oxidation.

The alkylbenzene-based mesophase pitch used in this study was limited in thermal stability to about 315°C, much lower than sketched in the process window of Fig. 3, but the fluidity at this temperature still permitted injection at acceptable pressure levels. Furthermore, injection runs at the lower temperature levels indicated that the preform was not adversely affected to viscosities as high as 200 Pa.s. Thus the processing window should be evaluated for each injection process in terms of the fiber weave and lay-up, the scale of the preform (*e.g.*, thin 2D

Table 2. Injection runs with plain-weave carbon fabric

Injection temperature (°C)	Injection pressure (kPa)	Ply thickness (microns)	Volume-% fiber (%)	Permeability (microns²)	Figure
321.5	69	209	46.5		7
316.3	110	204	47.6		7
311.9	107	198	49.1	0.60	7, 8A
309.0	97	237	45.5	3.0	8C
286.3	345	202	48.2	0.74	8B

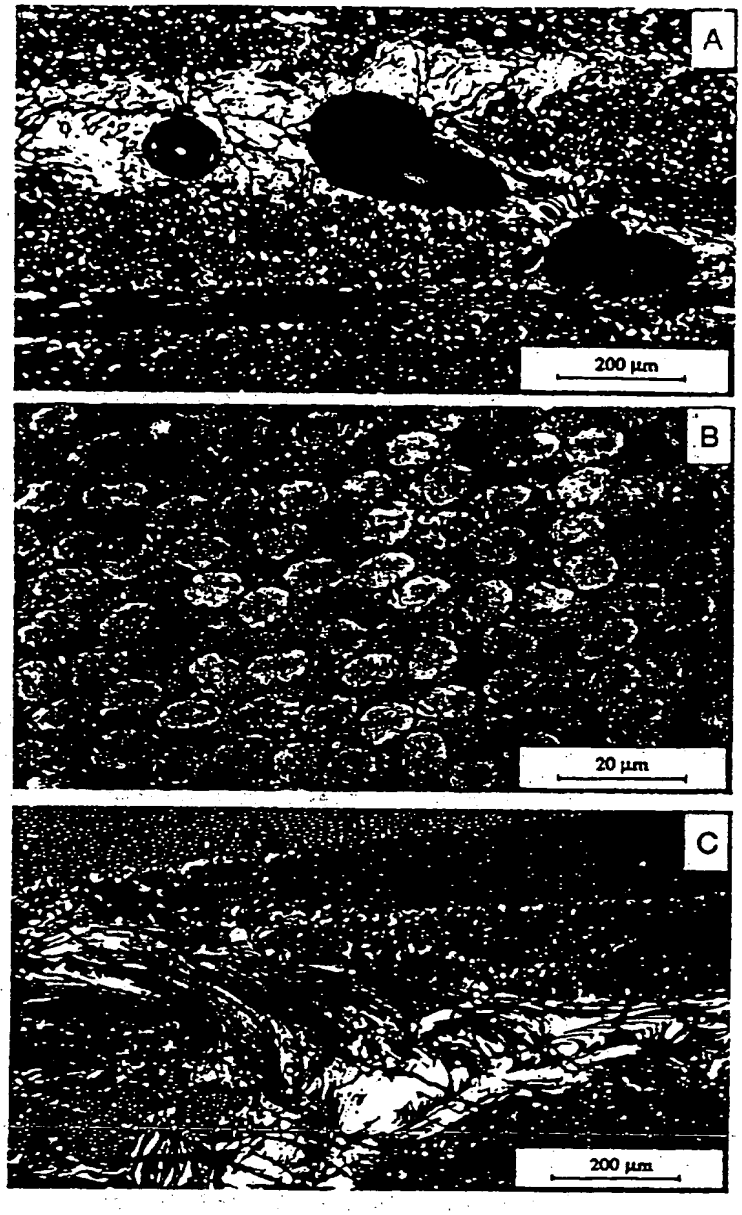

Fig. 8. Vertical micrographic sections through mesophase-injected preforms, viewed by cross polarizers: (A) Injected at 316°C: Bubbles are common in the flow channels between fiber bundles. (B) Injected at 309°C: Fiber bundles are well impregnated with mesophase. (C) Injected at 286°C: Bubbles are rare, both in channels and in fiber bundles.

panels or thick 3D blocks), as well as the flow properties of the candidate pitch.

Acknowledgments—We thank the Office of Naval Research for financial support and BP-America for an Extramural Research Award. We also thank Professor Stanley Middleman (UCSD) and L. H. Peebles, Jr. (ONR) for discussion and encouragement, J. E. Zimmer (Aerotherm Corp.) and K. Yanagida (Mitsubishi Oil) for provision of mesophase pitches, M. Tangen (ICI Fiberite) for provision of carbon fabric, and R. L. Weitz (Aerotherm Corp.) and P. M. Sheaffer (Aerospace Corp.) for assistance with micrographic preparation.

REFERENCES

1. L. S. Singer, *Carbon* 16, 408 (1978); see also U.S. Patent 4,005,183 (25 January 1977).
2. B. Rand, *Handbook of composites*; Vol 1: Strong fibers, (Edited by W. Watt and B. V. Pirov), Chap. 13, p 495. Elsevier (1985).
3. I. C. Lewis and F. F. Nazem, *Ext. Abstr., 18th Biennial Conf. Carbon*, Worcester, MA, p. 290 (1987).
4. Mitsubishi Oil Co.; see K. Yanagida, M. Noda, T. Sasaki, and K. Tate, *Ext. Abstr., 20th Biennial Conf. Carbon*, Santa Barbara, CA, p. 160 (1991).
5. A. Sakanishi, Y. Korai, I. Mochida, K. Yanagida, M. Noda, I. Thunori, and K. Tate, *Carbon* 30, 459 (1992).

6. Mitsubishi Gas–Chemical Co.; see I. Mochida *et al.*, *Carbon* 26, 843 (1988).
7. R. Fujiura, G. Kojima, K. Kanno, I. Mochida, and Y. Korai, *Carbon* 31, 97 (1993).
8. J. L. White and P. M. Sheaffer, *Carbon* 27, 697 (1989); *Carbon* 28, 235 (1990); see also P. M. Sheaffer and J. L. White, U.S. Patent 4,986,943 (22 January 1991).
9. K. Christ and K. J. Hüttinger, *Carbon* 31, 731 (1993).
10. J. L. White, *Ext. Abstr., 19th Biennial Conf. Carbon*, University Park, PA, p. 110 (1989).
11. J. L. White and M. K. Gopalakrishnan, *Ext. Abstr., 20th Biennial Conf. Carbon*, Santa Barbara, CA, p. 184 (1991).
12. B. Fathollahi, M. K. Gopalakrishnan, and J. L. White, *Carbon '92*, Proc. 5th Intl. Conf. on Carbon., p 36, Essen, Germany, 22–26 June 1992.
13. L. S. Singer, *Ext. Abstr., 19th Biennial Conf. Carbon*, University Park, PA, p. 146 (1989).
14. G. W. Collett and B. Rand, *Fuel* 57, 162 (1978).
15. R. Balduhn and E. Fitzer, *Carbon* 18, 155 (1980).
16. W. R. Hoffman and K. J. Hüttinger, *Carbon* 31, 263 (1993).
17. K.–J. Chen and R. J. Diefendorf, *CARBON '88*, Proc. Intl. Conf. on Carbon, Newcastle, U.K., p 16 (1988).
18. F. F. Nazem, *Fuel* 59, 851 (1980).
19. F. F. Nazem, *Carbon* 20, 345 (1982).
20. F. F. Nazem and I. C. Lewis, *Mol. Cryst. Liq. Cryst.* 139, 195 (1986).
21. E. Fitzer, D. Kompalik, and K. Yudate, *Fuel* 66, 1504 (1987).
22. K. Yamada, T. Imamura, M. Shibata, S. Arita, and H. Honda, *Proc. 10th Meeting, Carbon Society of Japan*, Paper All, p 22 (1983), in Japanese; summarized by S. Otani and A. Oya, In *Petroleum-Derived Carbons, Am. Chem. Soc. Symp. Series* 303, 323 (1986).
23. S. Chwastiak, U.S. Patent 4,209,500 (24 June 1980).
24. J. E. Zimmer, personal communication, 1989 (Aerotherm Corporation).
25. S. Chwastiak, R. T. Lewis, and J. D. Ruggiero, *Carbon* 19, 357 (1981).
26. J. L. White, *Petroleum-Derived Carbons, Am. Chem. Soc. Symp. Series* 21, 62 (1976).
27. J. E. Zimmer and J. L. White, *Carbon* 21, 323 (1983).
28. H. Brückmann, Dr.-Ing. thesis, Univ. Karlsruhe, Germany (1979); see E. Fitzer and A. Gkogkidis, In *Petroleum-Derived Carbons, Am. Chem. Soc. Symp. Series* 303, 369 (1986).